Audio Virtualization of Façade Acoustic Insulation by Convex Optimization

Alessandro Lapini
Department of Industrial Engineering
University of Florence
Florence, Italy
alessandro.lapini@unifi.it

Chiara Bartalucci
Department of Industrial Engineering
University of Florence
Florence, Italy
chiara.bartalucci@unifi.it

Francesco Borchi
Department of Industrial Engineering
University of Florence
Florence, Italy
francesco.borchi@unifi.it

Fabrizio Argenti
Department of Information Engineering
University of Florence
Florence, Italy
fabrizio.argenti@unifi.it

Monica Carfagni
Department of Industrial Engineering
University of Florence
Florence, Italy
monica.carfagni@unifi.it

***Abstract*—In this study, modeling of façade acoustic insulation is addressed. The objective is predicting the acoustic behaviour of a *virtual* façade on an incoming audio signal based on measurements made on an *actual* façade and on Standardized Level Differences (D_{nT}) curves known for both of them. In this way, a fast and concise characterization of acoustic insulation performance from outside noise can be achieved. The problem is cast as an inverse one, in which the acoustic impulse response of the actual façade must be substituted by the virtual one, taking into account, however, the constraints that are derived from the D_{nT} analysis. Experimental results are shown to demostrate the effectiveness of the proposed procedure.**

***Index Terms*—Audio virtualization, Acoustic insulation, Standardized Level Differences, Convex optimization**

I. Introduction

In system modeling, using direct and indirect measurements to infer the values of hidden or unobservable system parameters is usually referred to as an *inverse problem* [1]. Inverse problems arise in several engineering branches, such as biomedical imaging, optics, meteorology, and also audio processing. Incidentally, estimation of direction of arrival, blind source separation or computation of room impulse response are examples of inverse problems.

In this paper, the application of an inverse problem to the field of building acoustics is considered. This study focuses on the approximation of the acoustic insulation provided by a *virtual* façade on an audio signal that has been previously recorded in presence of an *actual*, generally different, façade. The problem can be cast as inverse because, in order to solve it, the contribution of the actual façade is substituted with the virtual one, relying uniquely on the knowledge of the *Standardized Level Difference* ($\mathrm{D_{nT}}$) [2]. $\mathrm{D_{nT}}$ curves are indirect and differential measurements of sound pressure level (SPL) carried out over prescribed frequency bands. They are extensively adopted in building acoustics for a fast and concise characterization of the acoustic insulation performance of a façade from outside noise. Nevertheless, to the best of authors' knowledge, this is the first work where they are used for the purpose of synthesis instead of analysis.

In the application considered here, the classical magnitude filter design cannot be used because of integral constraints on the magnitude of the frequency response that need to be enforced. Thus, a solution based on convex optimization [3] is explored. Magnitude filter design by convex optimization has been already investigated in the literature, considering approaches relying on linear programming [4], semidefinite programming [5], [6], linear matrix inequalities [7] and directed iterative rank refinement [8]. Unfortunately, such methods cannot be directly applied in the context of this study due to the particular modeling of the problem. Nevertheless, ideas proposed in those works have been exploited to approximate our problem and to solve it by standard convex optimization routines.

The remainder of the paper is structured as follows. The formal modeling of the problem is presented Section II. The proposed method is described in Section III. Experimental results are shown in Section IV, whereas conclusions are drawn in Section V.

II. Problem modeling

In this Section, the model of the considered scenario is introduced and the goal is formalized.

Accordingly to Figure 1, the acoustic signal x' generated by a source located *outside* a building is recorded by a microphone placed *inside* it, providing the audio signal y_a. The whole system is assumed linear and time–invariant; hence, the input-output relation is given by the following discrete linear convolution:

$$\begin{aligned} y_a[n] &= x'[n] * g[n] * h_a[n] \\ &= x[n] * h_a[n], \end{aligned} \quad (1)$$

where h_a is the impulse response of the filter modeling the actual façade and g is the filter accounting for the remaining acoustic effects (e.g. free-space loss, reverberation). In other words, the signal x indicates the recorded acoustic signal after the contribution of h_a were removed.

By assuming that the actual façade were replaced by the virtual one, the virtual signal y_v that would be recorded is

$$y_v[n] = x[n] * h_v[n], \quad (2)$$

ISBN 978-90-827970-1-5

being h_v the impulse response of the filter modeling the virtual façade. Substituting (1) into (2), the virtual signal is theoretically provided by

$$y_v[n] = y_a[n] * h_a^{-1}[n] * h_v[n]\,, \tag{3}$$

that is, the target signal can be obtained by inverse and direct filtering the recorded signal by means of the actual and virtual façade filters, respectively. It has to be noted that $\{h_a, h_v\}$ generally depend upon several parameters, e.g., the position and the directivity of both the source and receiver, the façade's and building's geometry and materials; thus, aggregate parameters like $\mathrm{D_{nT}}$ are commonly preferred for the analysis and the comparison of façades' insulating performance.

There exists a standard procedure to evaluate the $\mathrm{D_{nT}}$ curves of façades [2], which can be qualitatively approximated as an average of multiple SPL measurements carried out across several positions inside and outside the building. Therefore, an accurate theoretical model that relates all the measurements to the $\mathrm{D_{nT}}$ curves is of difficult formalization and beyond the scope of this work.

In this paper, a simplified modeling is used. The $\mathrm{D_{nT}}$ curve is considered as evaluated through a single measurement, according to the setup depicted in Figure 2. The $\mathrm{D_{nT}}$ value in the frequency band Δ_m, shortly $D_m^{(a)}$, is computed as the ratio between the energies of the signals recorded by two distinct microphones suitably placed outside and inside the actual façade, respectively, in the presence of an external pink noise source. The power spectral density of the pink noise is assumed to be σ/F, where σ is a constant. By neglecting other sources of disturbance, $D_n^{(a)}$ can be approximated as the ratio of integrated power spectral densities, i.e.

$$D_m^{(a)} \approx \frac{\int_{\Delta_m} \sigma F^{-1}\,\mathrm{d}F}{\int_{\Delta_m} \sigma F^{-1}|H_a(F)|^2\,\mathrm{d}F} = \frac{\int_{\Delta_m} F^{-1}\,\mathrm{d}F}{\int_{\Delta_m} F^{-1}|H_a(F)|^2\,\mathrm{d}F} \qquad m = 1,\dots M\,, \tag{4}$$

where H_a is the Fourier transform of h_a; $m = 1,\dots M$ indexes the set of frequency bands which the $\mathrm{D_{nT}}$ values are computed over. An analogous procedure is performed to obtain the $\mathrm{D_{nT}}$ curve of the virtual façade, namely $D_m^{(v)}$, over the same bands.

$\mathrm{D_{nT}}$ curves do not cover the entire range $[0, F_s]$, being F_s the sampling frequency [2]; hence, $\overline{M}$ complementary bands $\overline{\Delta}_m$ are introduced, that is,

$$\overline{\Delta}_m \cap \bigcup_{p=1}^{M} \Delta_p = \emptyset \qquad m = 1,\dots,\overline{M}$$

such that

$$\bigcup_{m=1}^{M} \Delta_m \cup \bigcup_{m=1}^{\overline{M}} \overline{\Delta}_m \equiv [0, F_s]\,.$$

By considering (3) and (4), the goal is formally defined as follows: synthesize

$$\hat{y}_v[n] = y_a[n] * \hat{h}_a^{-1}[n] * \hat{h}_v[n]. \tag{5}$$

where the estimated filters $\{\hat{h}_a, \hat{h}_v\}$ are constrained by

$$\int_{\Delta_m} F^{-1}|\hat{H}_a(F)|^2\,\mathrm{d}F = \frac{\int_{\Delta_m} F^{-1}\,\mathrm{d}F}{D_m^{(a)}}, \quad m = 1,\dots M \tag{6}$$

$$\int_{\Delta_m} F^{-1}|\hat{H}_v(F)|^2\,\mathrm{d}F = \frac{\int_{\Delta_m} F^{-1}\,\mathrm{d}F}{D_m^{(v)}}, \quad m = 1,\dots M \tag{7}$$

$$\hat{H}_a(F) = \hat{H}_v(F), \quad \forall F \in \bigcup_{m=1}^{\overline{M}} \overline{\Delta}_m \tag{8}$$

$$\angle\hat{H}_a(F) = \angle\hat{H}_v(F), \quad \forall F \in [0, F_s]\,. \tag{9}$$

The above equations represent a non–convex set of integral, semi–infinite and phase constraints. Equations (6)–(7) come from (4) and enforce the similarity to the measured data; (8) ensures that the synthesized signal adheres to the recorded one for all the frequencies, even where no information is available; (9) prevents phase distortions between $\hat{y}_v$ and y_v. In case of ideal estimation, i.e., $\hat{h}_a = h_a$ and $\hat{h}_v = h_v$, (5) and (3) consistently coincide.

III. Proposed method

The proposed procedure is iterative: at each iteration a convex optimization problem and a spectral factorization have to be solved; the termination condition is achieved when the estimated filters sufficiently adhere to the acquired data. The algorithm, which is summarized in Algorithm 1, is described in the following.

The autocorrelation sequence of the actual façade, $\hat{r}_a$, and the related power spectral density $\hat{R}_a$ are defined, respectively, as

$$\hat{r}_a[n] = \hat{h}_a[n] * \hat{h}_a[-n] \tag{10}$$

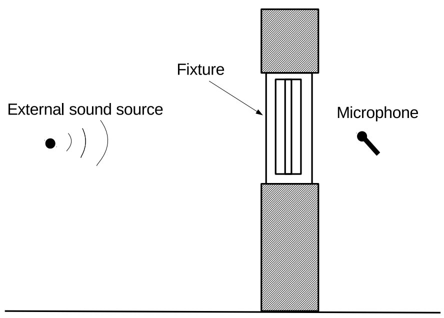

Fig. 1: Schematic view of the recording scenario.

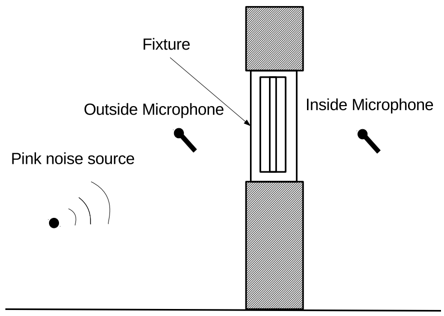

Fig. 2: Schematic view of the measurement setup of $\mathrm{D_{nT}}$ curves.

$$\hat{R}_a(F) = |\hat{H}_a(F)|^2 \quad (11)$$

$$= \hat{r}_a[0] + 2\sum_{n=1}^{N-1} \hat{r}_a[n]\cos(2\pi F n) \quad (12)$$

where N is the filter length, with N odd. Analogously, $\hat{r}_v$ and $\hat{R}_v$ are defined for the virtual façade. Moreover, the following quantities are introduced:

$$L_n(F) = \begin{cases} 1 & \text{for } n = 0 \\ 2\cos(2\pi F n) & \text{otherwise} \end{cases} \quad (13)$$

$$C_{n,m} = \frac{D_m^{(a)} \int_{\Delta_m} F^{-1} L_n(F)\, \mathrm{d}F}{\int_{\Delta_m} F^{-1}\, \mathrm{d}F}\,, \quad (14)$$

as well as the tolerances ϵ_0 and α_0 ($\epsilon_0 > 1$, $\alpha_0 > 0$). Equation (8) is relaxed into $\hat{R}_a = \hat{R}_v$. According to the previous definitions, (6)–(8) are approximated with the following finite set of convex constraints:

$$\frac{1}{\epsilon} \le \sum_{n=0}^{\lceil N/4\rceil-1} \hat{r}_a[n] C_{n,m} \le \epsilon, \quad m = 1, \dots M \quad (15)$$

$$\frac{1}{\epsilon} \le \sum_{n=0}^{\lceil N/4\rceil-1} \hat{r}_v[n] C_{n,m} \le \epsilon, \quad m = 1, \dots M \quad (16)$$

$$\frac{1}{\epsilon} \le \frac{\sum_{n=0}^{\lceil N/4\rceil-1} \hat{r}_v[n] L_n(F_i)}{\sum_{n=0}^{\lceil N/4\rceil-1} \hat{r}_a[n] L_n(F_i)} \le \epsilon,$$

$$F_i \in \bigcup_{m=1}^{\overline{M}} \overline{\Delta}_m,\ i = 1, \dots P_m \quad (17)$$

$$\alpha_0 \le \sum_{n=0}^{\lceil N/4\rceil-1} \hat{r}_a[n] L_n(F_j),\ F_j \in [0, F_s],\ j = 1, \dots Q \quad (18)$$

$$\alpha_0 \le \sum_{n=0}^{\lceil N/4\rceil-1} \hat{r}_v[n] L_n(F_j),\ F_j \in [0, F_s],\ j = 1, \dots Q\,, \quad (19)$$

where F_i and F_j are frequencies over the complementary bands and over the entire spectrum, respectively, and $\epsilon = \epsilon_0$ at the first iteration. Inequalities (15)–(16) are derived from (6)–(7) by substituting (11)–(13), respectively, and introducing the tolerance bounds. Similarly, (17) is the discrete–frequency version[1] of (8), having replaced the filters' frequency responses with their power spectral densities. Inequalities (18)–(19) enforce the positiveness of the power spectral densities [4], [5].

The goal of our method would be achieving a smooth $\hat{R}_v/\hat{R}_a$, constrained by relations (15)–(19). This could be obtained by minimizing the energy of the derivative of $\hat{R}_v/\hat{R}_a$, but this leads to a nonconvex problem. Therefore, we resort to a different approach aiming to smooth both the numerator and the denominator of the above ratio. Thus, a weighted sum of the energy of the derivatives of such terms is considered. Applying the Parseval's theorem, it can be shown that the goal can be formalized as a convex problem with respect to $\{\hat{r}_a, \hat{r}_v\}$, given by

$$\text{minimize} \sum_{n=0}^{\lceil N/4\rceil-1} n^2 \left(\frac{\hat{r}_a[n]}{W_a} + \frac{\hat{r}_v[n]}{W_v}\right)^2$$

$$\text{subject to (15)–(19)}\,, \quad (20)$$

where

$$W_a = \sum_{m=1}^{M-1} \left| \frac{\int_{\Delta_{m+1}} F^{-1}\, \mathrm{d}F}{D_{m+1}^{(a)}} - \frac{\int_{\Delta_m} F^{-1}\, \mathrm{d}F}{D_m^{(a)}} \right|$$

$$W_v = \sum_{m=1}^{M-1} \left| \frac{\int_{\Delta_{m+1}} F^{-1}\, \mathrm{d}F}{D_{m+1}^{(v)}} - \frac{\int_{\Delta_m} F^{-1}\, \mathrm{d}F}{D_m^{(v)}} \right|.$$

It has to be noted that in (15)–(20), the autocorrelation sequence is truncated at $\lceil N/4\rceil - 1$ to limit the computational burden of the convex optimization procedure. Furthermore, the problem (20) might generally result unfeasible for the given N; in such a case, it is iteratively solved by increasing N until a valid solution is achieved.

After solving (20), the phase constraint (9) has to be enforced. Equation (9) is strengthened by assuming

$$\angle \hat{H}_a(F) = \angle \hat{H}_v(F) = 0, \quad \forall F\,, \quad (21)$$

i.e., zero–phase filters, which implies that there exist two causal sequences $\{\hat{b}_a, \hat{b}_v\}$ of length $\lceil N/2\rceil$ such that

$$\begin{aligned} \hat{h}_a[n] &= \hat{b}_a[n] * \hat{b}_a[-n] \\ \hat{h}_v[n] &= \hat{b}_v[n] * \hat{b}_v[-n]\,. \end{aligned} \quad (22)$$

Substituting (22) into (10) and recursively into (11), after taking the logarithm, yields

$$\begin{aligned} 4\ln|\hat{B}_a(F)| &= \ln \hat{R}_a(F) \\ 4\ln|\hat{B}_v(F)| &= \ln \hat{R}_v(F)\,. \end{aligned} \quad (23)$$

Replacing (23) in the approximation of real cepstrum [9], i.e.

$$\tilde{b}[n] = \text{IFFT}\{\ln|\hat{B}(F)|\}\,,$$

where IFFT$\{\cdot\}$ is the Inverse Fast Fourier Transform, the real cepstra of $(\hat{b}_a, \hat{b}_v)$ are approximated by

$$\begin{aligned} \tilde{b}_a[n] &= \text{IFFT}\{\ln|\hat{R}_a(F)/4|\} \\ \tilde{b}_v[n] &= \text{IFFT}\{\ln|\hat{R}_v(F)/4|\}\,. \end{aligned} \quad (24)$$

Therefore, $\{\hat{h}_a, \hat{h}_v\}$ are computed by means of the following spectral factorization: after computing the real cepstra $\{\tilde{b}_a, \tilde{b}_v\}$ through (24), $\{\hat{b}_a, \hat{b}_v\}$ are synthesized by means of minimum phase reconstruction [4], [10][2]

$$\begin{aligned} \hat{b}_a[n] &= \text{Re}\,\text{IFFT}\{\exp(\text{FFT}\{\tilde{b}_a[n]\,w[n]\})\} \\ \hat{b}_v[n] &= \text{Re}\,\text{IFFT}\{\exp(\text{FFT}\{\tilde{b}_v[n]\,w[n]\})\}\,, \end{aligned} \quad (25)$$

being

$$w[n] = \begin{cases} 0\,, & \text{for } n < 0 \\ 1\,, & \text{for } n = 0 \\ 2\,, & \text{otherwise}\,, \end{cases}$$

and $\{\hat{h}_a, \hat{h}_v\}$ are eventually computed according to (22).

The solution obtained after the first iteration may not fulfill the integral constraints due to the approximation introduced by the spectral factorization [4]. Thus, the

[1]The convexity is implicit for sake of brevity.

[2]The procedure proposed in [11] can be used as alternative.

ISBN 978-90-827970-1-5

whole procedure is iterated by decreasing ϵ, until the following inequalities are satisfied:

$$\begin{aligned} \frac{1}{\epsilon_0} \le \sum_{n=0}^{N-1} \hat{r}_a[n] C_{n,m} \le \epsilon_0, \quad m = 1, \dots M \\ \frac{1}{\epsilon_0} \le \sum_{n=0}^{N-1} \hat{r}_v[n] C_{n,m} \le \epsilon_0, \quad m = 1, \dots M\,. \end{aligned} \tag{26}$$

Algorithm 1 Procedure of the proposed method

Input: N odd, $\epsilon_0 > 1$, $\alpha_0 > 0$, y_a, $\{D_m^{(a)}, D_m^{(v)}\}$ for $m = 1, \dots M$

Output: $\hat{y}_v$, $\{\hat{h}_a, \hat{h}_v\}$

$\epsilon \leftarrow \epsilon_0$
repeat
  while (20) is unfeasible **do**
    increase N
  end while
  compute $\{\hat{r}_a, \hat{r}_v\}$ by solving (20)
  compute real cepstra $\{\tilde{b}_a, \tilde{b}_v\}$ by means of (24)
  compute $\{\hat{b}_a, \hat{b}_v\}$ through (25)
  compute $\{\hat{h}_a, \hat{h}_v\}$ by means of (22)
  decrease ϵ
until (26) is satisfied
compute $\hat{y}_v$ by means of (5)

IV. Results

The proposed method has been tested by selecting one low–performance façade as the actual one, whose D_{nT} has been directly measured. Four façades have been chosen as the virtual ones. The D_{nT} curves of virtual façades have been determined according to [12] starting from sound insulation measurements of high performance fixtures carried out in laboratory [13]. All curves have been accordingly reported over one–third octave bands, as depicted in Figure 3, where their nominal central frequencies are reported. The lowest and the highest one–third bands have nominal central frequency equal to 50 and 3150 Hz, respectively; the total number of bands is $M = 19$. A pair of complementary bands ($\overline{M} = 2$) are set between 0 and 44 Hz (i.e. the lower bound of the lowest band) and between 3563 Hz (i.e. the upper bound of the highest band) and 4000 Hz. The sampling frequency is $F_s = 8000$ Hz. As to the tolerances, ϵ_0 and α_0 are set to 0.1 dB and -110 dB, respectively.

In order to provide a homogeneous distribution, the number of sampling points P_m for each complementary band is set to

$$P_m = \frac{30N|\Delta_m|}{F_s}\,,$$

being $|\Delta_m|$ the bandwidth of Δ_m, whereas Q is set to $30N$.

The filters $\{\hat{h}_a, \hat{h}_v\}$ for all the considered scenarios have been successfully synthesized by using a filter length $N = 2047$. For the convex optimization, the CVX [14], [15], a package for specifying and solving convex programs, and the MOSEK solver have been used in the MATLAB environment. The magnitude of the frequency response of the synthesized filters, as well as of the equivalent filter

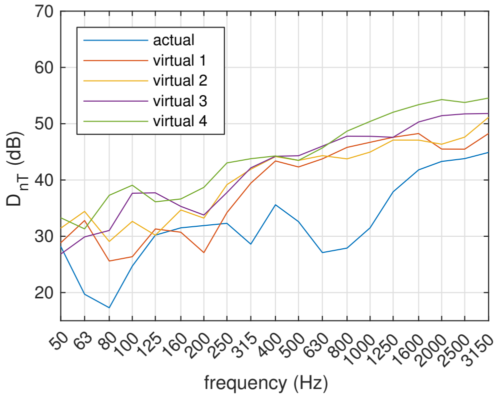

Fig. 3: D_{nT} curves of the actual and virtual façades.

H_v/H_a, are reported in Figure 4. The synthesized filters exhibit a smooth profile in the one–third octave bands, especially in the lower part of the spectrum, providing a regular behavior across different scales. The equivalent filter provides a 0 dB response in the complementary bands thanks to the fact that H_a ans H_v nearly coincide in such frequency regions. Furthermore, the ripple of H_a is conveniently limited in the third–octave bands, avoiding the outbreak of resonance peaks in the frequency response of the equivalent filters.

V. Conclusions

A novel method for the virtualization of the façade's effect on an audio signal has been presented. The proposed procedure relies on a simplified signal model that, by only requiring the knowledge of the Standardized Level Difference curves, replaces the acoustic effect provided by an actual façade on a recorded signal with the acoustic effect of a virtual façade. The filters modeling the façades' effects are estimated by means of convex optimization and spectral factorization techniques in order to satisfy the measured data. The procedure has been also shown to successfully manage the presence of no–information bands, which is a common scenario in measured insulation curves, by synthesizing a flat passband response in such regions. Furthermore, the lack of phase information is dealt with by resorting on zero–phase direct and inverse filtering, providing no phase distortion in the output signal. The validation of the proposed algorithm with signals acquired in presence of the virtual façades will be possibly investigated in future works.

References

[1] A. Tarantola, *Inverse Problem Theory and Methods for Model Parameter Estimation*. Society for Industrial and Applied Mathematics, 2005. [Online]. Available: http://epubs.siam.org/doi/abs/10.1137/1.9780898717921

[2] "Acoustics — field measurement of sound insulation in buildings and of building elements — part 3: Façade sound insulation," ISO 16283-3:2016(en), Feb. 2016.

[3] S. Boyd and L. Vandenberghe, *Convex Optimization*. New York, NY, USA: Cambridge University Press, 2004.

[4] S.-P. Wu, S. Boyd, and L. Vandenberghe, *FIR Filter Design via Spectral Factorization and Convex Optimization*. Boston, MA: Birkhäuser Boston, 1999, pp. 215–245.

[5] ——, "Fir filter design via semidefinite programming and spectral factorization," in *Proceedings of 35th IEEE Conference on Decision and Control*, vol. 1, Dec 1996, pp. 271–276 vol.1.

ISBN 978-90-827970-1-5 © EURASIP 2018

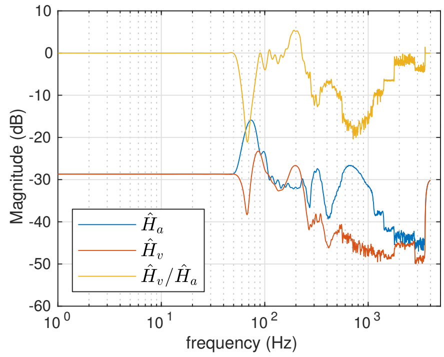

(a)

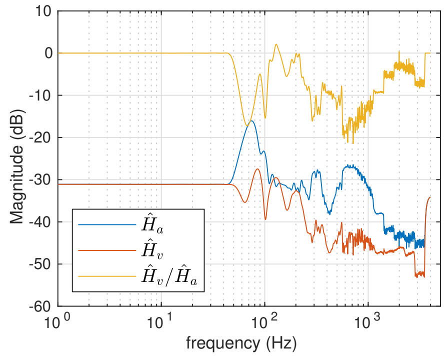

(b)

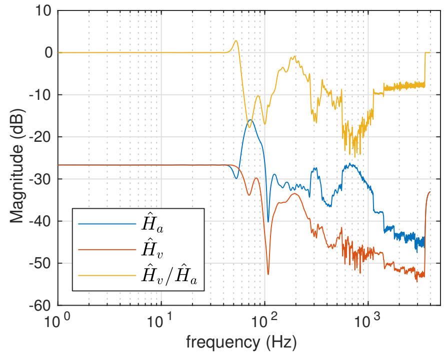

(c)

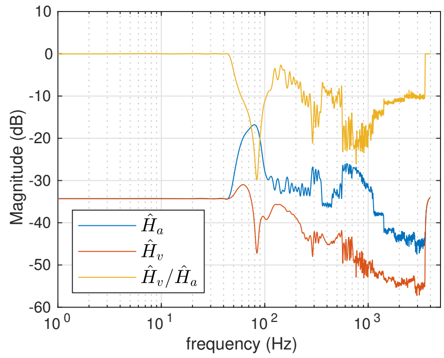

(d)

Fig. 4: Frequency response of the synthesized filters for the virtual façades 1–4 (a–d).

[6] B. Alkire and L. Vandenberghe, "Convex optimization problems involving finite autocorrelation sequences," *Mathematical Programming*, vol. 93, no. 3, pp. 331–359, Dec 2002.

[7] T. N. Davidson, Z.-Q. Luo, and J. F. Sturm, "Linear matrix inequality formulation of spectral mask constraints with applications to fir filter design," *IEEE Transactions on Signal Processing*, vol. 50, no. 11, pp. 2702–2715, Nov 2002.

[8] M. Dedeoğlu, Y. K. Alp, and O. Arıkan, "Fir filter design by convex optimization using directed iterative rank refinement algorithm," *IEEE Transactions on Signal Processing*, vol. 64, no. 9, pp. 2209–2219, May 2016.

[9] A. V. Oppenheim and R. W. Schafer, *Discrete-Time Signal Processing*, 3rd ed. Upper Saddle River, NJ, USA: Prentice Hall Press, 2009.

[10] D. S. P. Committe, *Programs for Digital Signal Processing*. Piscataway, NJ, USA: IEEE Press, 1979.

[11] S. C. Pei and H. S. Lin, "Minimum-phase fir filter design using real cepstrum," *IEEE Transactions on Circuits and Systems II: Express Briefs*, vol. 53, no. 10, pp. 1113–1117, Oct 2006.

[12] "Building acoustics – estimation of acoustic performance of buildings from the performance of elements – part 3: Airborne sound insulation against outdoor sound," ISO 12354-3:2017(en), Jul. 2017.

[13] "Acoustics – laboratory measurement of sound insulation of building elements – part 2: Measurement of airborne sound insulation," ISO 10140-2:2010(en), Sep. 2010.

[14] M. Grant and S. Boyd, "Graph implementations for nonsmooth convex programs," in *Recent Advances in Learning and Control*, ser. Lecture Notes in Control and Information Sciences, V. Blondel, S. Boyd, and H. Kimura, Eds. Springer-Verlag Limited, 2008, pp. 95–110.

[15] ——, "CVX: Matlab software for disciplined convex programming, version 2.1," http://cvxr.com/cvx, Mar. 2014.

ISBN 978-90-827970-1-5 © EURASIP 2018